Computational Models of Brain Connectivity from Diffusion Weighted Images

Description of Proposal

Diffusion Weighted Magnetic Resonance Imaging (DWI) enables the exploration of fibrous tissues such as brain white matter and muscles non-invasively *in-vivo*. It exploits the fact that water in these tissues diffuses at faster rates along fibers than orthogonal to them. Integral curves that estimate the geometry of fiber tracts by showing paths of fastest diffusion are among the most common information derived from DWI volumes. The relation between the state of diffusivity in the brain and the health of the brain has been long established with several studies. This is only natural given the fact that diffusion provides a non-invasive probe into the micro-architecture of the white matter and that neuro-degenerative diseases/injuries such as multiple sclerosis(MS), Vascular Cognitive Impairment (VCI), Amyotrophic Lateral Sclerosis (ALS), Alzhemeir's disease, HIV-associated dementia, Cerebral Autosomal Dominant Arteriopathy with Subcortical Infarcts and Leukoencephalopathy (CADASIL), and concussions affect the structure of the white-matter connectivity (i.e., size, shape, length, number of axons).

In this context, we propose to develop computational models for exploring and understanding the structure and pattern of the connectivity in the brain using DWI. The underlying premise of our approach is to characterize connectivity both qualitatively and quantitatively. We identify a set of connectivity-related problems and then propose our solutions. Our proposed solutions use new as well as well-known ideas from statistical machine learning, geometry and topology; while statistics and metric geometry will be important in quantitative modeling, topology, particularly homology, will help capture qualitative aspects of the connectivity. Our contributions include automatic generation of two-dimensional connectivity maps of the brain, the real projective plane ($\boldsymbol{RP^2}$) as the model of the connectivity, resolving fiber crossings with model selection, construction of the topological skeleton of tensor fields using Reeb graphs, and characterization of tensor fields with topological invariants such as Betti numbers. We will demonstrate utility of our methods in understanding normal and pathological variation in the connectivity of the brain. There is a large body of work in understanding the connectivity of the brain at cellular and microscopic levels. Therefore, the proposed work will be complementary to these previous and ongoing efforts in scale (i.e., in comparison to optical imaging, DWI provides a coarser view of the connectivity). While our research will be carried out with applications to the human brain in mind, the results will likely have broader implications, as the ability to characterize and visualize connectivity, based on different domain specific "metric" and "non-metric" criteria, is important in understanding any given abstract or scientific data.

Research Plan

A Specific Aims

We propose to address a set of problems that appear in extracting, analyzing, and visualizing connectivity information from DWI brain data sets. The recurring idea in our proposed solutions is to characterize the structure and pattern of connectivity both qualitatively and quantitatively at varying scales. In doing so, we will develop new methods as well as use existing tools from statistical machine learning, geometry and topology [56, 13, 16, 24, 47]. In the rest of this section we summarize five different proposal ideas with a list of related actions without a complete discussion. For details of the concepts, the reader will need to refer to the background section B.

A.1 Two-dimensional Maps of Connectivity in the Brain

We propose to automatically generate two-dimensional connectivity maps from DWI brain data sets. While a three-dimensional graph of the core of the brain, where nodes are restricted to the cortex, has been computed in

the past for network analysis [33], general two-dimensional maps have not been computed and used for visualization and modeling purposes. A two-dimensional hierarchical "circuit diagram" will provide an effective model to study as well as visualize the brain connectivity. In order to embed paths into a plane with different scale hierarchies while obeying a set of constraints, we will use robust similarity metrics, clustering, and tools from calculus of variations.

We will

- create a two-dimensional connectivity diagram for clustered fiber tracts obtained from a normal DWI brain data set by embedding the end-point regions of the clusters and the centroid paths into the plane,
- link this 2d representation with the 3d fiber tract and cortex surface in an interactive tool, and
- run a user-study to compare the proposed model with the current standard in exploring and visualizing the white matter connectivity in the brain.

A.2 The Real Projective Plane as Model of Connectivity

The tensor model (DTI:Diffusion-Tensor MRI) is the most common model of diffusivity provided by DWI, where diffusivity at each voxel is represented with a single symmetric second-order tensor. Principal axes of tensors in a second order tensor field constitute a line field. Therefore integral curves estimating fiber tracts by showing paths of fastest diffusion are essentially results of integration over line fields. Since the space of three dimensional lines is identical to $\boldsymbol{RP^2}$(i.e., every point on $\boldsymbol{RP^2}$determines a line and vice versa), we propose to use $\boldsymbol{RP^2}$as a geometric model of connectivity. Among other things, this will provide a formalism to visualize and study connectivity through a well-known geometry.

We will

- visualize line fields using $\boldsymbol{RP^2}$immersions, including Boy's surface,
- characterize these immersions by relating them to variational methods (i.e., compute "distances" between lines and embed them in a color space, for example, using ℓ_1 norm),
- evaluate effectiveness coloring based on $\boldsymbol{RP^2}$immersions and variational methods, and
- perform critical point analysis of fiber tracts on $\boldsymbol{RP^2}$, similar to what has been done in crystallographic topology, and compare the results with the current state of the art in critical point analysis of diffusion tensor fields.

A.3 Bayesian Resolving of Path Crossings

While the single symmetric tensor model of diffusion provides a simple and tractable way of estimating fiber tract geometries, it fails to resolve crossing(X), branching(-<) and kissing(><) behaviors of fiber tracts. In order to compute the "sufficient" number of tensors at each voxel, we propose to pose the problem as a simple, coarse to fine, Bayesian model selection problem and solve it using a hierarchical Markov Random Field model.

We will

- validate the proposed technique first for a synthetic data
- and then for the optic chiasm in the brain, which embodies both branching and crossing behaviors, as in done some previous work (e.g, [43]).

A.4 Reeb Graphs of Tensor Fields

Reeb graph of a function $f : M \rightarrow R$ defined over a manifold M provides an efficient representation of how level sets of f evolve and as well as hints of the topology of the space (i.e., global structure) on which f is defined [56]. Formally, suppose that we have an equivalence relation $\sim$ defined on the manifold M such that $x \sim y$ if only if $f(x) = f(y)$. Then the Reeb graph of f is the quotient space $M_{\sim}$ defined by this equivalence relation. We propose to compute Reeb graphs of diffusion tensor invariants, which are scalar functions. We also aim to generalize Reeb graphs to vector-valued functions defined over manifolds so that we can compute, for example, Reeb graphs of symmetric second order tensor fields (i.e., 6-dimensional functions over 3-manifolds with boundary in our case) directly.

We will

- compute Reeb graphs of scalar tensor invariants such as fractional anisotropy (FA) and mean diffusivity (MD) in the corpus callosum (CC).
- quantify stability of the topology by computing Reeb graphs at different scales and varying parameter settings,
- visualize the persistence of the topological skeletons.
- validate computed Reeb graphs with the white matter segmentation results.
- compare the results with other skeletonization methods of tensor fields.

A.5 Computational Homology of Tensor Fields

We propose to qualitatively determine the structure and pattern in the brain white matter connectivity using homology. For this, we will compute and compare topological invariants such as Betti numbers (counters of ranks of n-dimensional cycle groups) over data sets.

We will

- compute Betti numbers for the CC.
- quantify the variation of Betti numbers from a healthy brain to diseased brain, and
- compare Betti numbers with other markers, such as FA and MD, in quantifying neurodegenerative disorders including VCI, CADASIL, HIV and MS.

B Significance & Background

Most of the ideas in this proposal have been formed having applications to the brain connectivity in mind. In this context, we first give a background on DWI that would be sufficient to follow the rest of the proposal. Then we sample from the existing body of work relating to proposed ideas introduced in Section A.

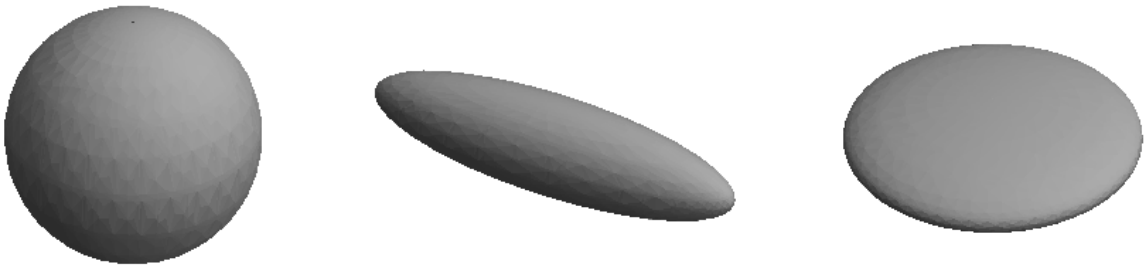

$\lambda_1 = \lambda_2 = \lambda_3$ $\lambda_1 > \lambda_2 = \lambda_3$ $\lambda_1 = \lambda_2 > \lambda_3$

Figure 1: *Three configurations of tensor ellipsoids.* $\lambda_1, \lambda_2, \lambda_3$ *correspond to lengths of the longest, median and shortest semi-axes of the ellipsoid. They also represent the eigenvalues of the corresponding diffusion tensor. Similarly, the directions of the semi-axes of the ellipsoid represent the eigenvectors of the corresponding diffusion tensor.*

B.1 DWI

DWI provides a way to measure microarchitecture of fibrous tissues induced by the Brownian motion of water molecules. Compare to conventional MRI, diffusion MRI provides much richer anatomical information about the white matter structure in the brain (the white matter looks homogeneous on conventional MRI). It is also unique among imaging techniques in being no-invasive, and inherently three-dimensional. There have been mainly two diffusion models proposed; The first was diffusion tensor (DT) and more recently q-ball. The process of fitting a single second-order symmetric tensor D at each voxel to DWI measurements is called diffusion tensor MRI (DTI).

$$D = \begin{pmatrix} D_{xx} & D_{xy} & D_{xz} \\ D_{yx} & D_{yy} & D_{yz} \\ D_{zx} & D_{zy} & D_{zz} \end{pmatrix}$$

Conveniently, a given diffusion tensor also determines an ellipsoid uniquely (i.e., $x^t D x = 1$); so we can visualize diffusion tensors with the corresponding ellipsoids. Consequently, major axes of the ellipsoid and corresponding radii also represent direction of major diffusion axes (eigenvectors of D) and diffusion rates (eigenvalues of D; see Figure 1). The most common measures are the mean diffusivity (MD) and fractional anisotropy (FA). Both measures are simple statistics over the eigenvalues of D. While MD is the mean of the eigenvalues, FA corresponds to the standard deviation of the normalized eigenvalues. While higher MD values denote higher diffusivity, FA is an anisotropy measure, quantifying the extent with which the diffusion tensor deviates from being isotropic [11].Values of FA range from 0 to 1.

$$\mathsf{MD} = \frac{\lambda_1 + \lambda_2 + \lambda_3}{3}$$

$$\mathsf{FA} = \frac{\sqrt{3}}{\sqrt{2}} \sqrt{\frac{((\lambda_1 - \mathsf{MD})^2 + (\lambda_2 - \mathsf{MD})^2 + (\lambda_3 - \mathsf{MD})^2)}{\left(\lambda_1^2 + \lambda_2^2 + \lambda_3^2\right)}}$$

We will primarily use DTI data sets for estimating the geometry of the connectivity in the brain.

Starting in the second half of the 1990s, use of DTI in clinical research, which includes diagnosing and monitoring various neural disorders, and in neuroscience research has flourished. There are good reviews on theoretical and practical underpinnings of DTI data acquisition, processing, and applications [5, 50].

B.1.1 Applications of DTI

Clinical relevance of diffusivity in the brain has been established with several studies. One of the earliest and arguably the most successful clinical application of diffusion MRI has been the brain ischemia. Moseley et al. found that diffusion drops at a very early stage of the ischemia in cat brain [51]. Diffusion MRI provides some patients with the opportunity to receive suitable treatment at a stage when brain tissue might still be salvageable. In general, DTI has found applications in all neurodegenerative diseases affecting the white-matter integrity such as multiple sclerosis [39, 70], , CADASIL [19, 49], ALS [26, 32, 58], Alzhemeir's disease [34, 23, 57]., and HIV[27, 54, 55]. In addition to clinical applications, DTI has been increasingly used in neuroscience research. Examples include phenotype characterization [73, 68], brain development [52, 74] and white matter segmentation and visualization of connectivity [18, 6]. Tractography has been increasingly used in neuroscience studies exploring white matter connectivity, effects of pathologies on connectivity, and improvement of data acquisition and visualization methods. Quantitative tractography methods can represent complex 3D geometric and integrity characteristics of white matter features with scalar measurements so that the microstructural integrity of entire tracts of interest (TOI) can be assessed. We believe, they have potential for helping to assess the cognitive and functional impact of disease-related injury to specific white matter pathways.

B.2 Automatic Generation of Brain Networks

Efforts to create representations (often spatial) of anatomical and functional structures of the brain and their interrelations at different scales in the brain (a.k.a. brain mapping) have been focus of research in last two decades. To this end, various image modalities, including EEG, structural MRI, fMRI have been used. DWI provides a unique window into the white matter structure in the brain.

Previous attempts to provide a map of structural connections of the human brain have utilized correlations in cortical gray-matter thickness [36] as well as DTI [40, 41]. Recently DWI has been used to map the connectivity of the structural core of the brain, where nodes are restricted to only the cortical regions [33]. Our method will create planar embeddings of the pathways that satisfy a set of anatomical and visual constraints.

B.3 Real Projective Plane as a Model of Line Fields

The real projective plane ($\boldsymbol{RP^2}$) is the set of lines through the origin in R^3; this set corresponds naturally to a surface. There are several ways to describe this surface; we show the most common ones in Figure 2.

In DTI, integral curve estimates of the fiber tracts in the brain are obtained integrating along the field of principal eigenvectors of the tensors. The field of eigenvectors of diffusion tensor is indeed a line field because diffusion is spatially symmetric; if $\mathbf{v}$ is an eigenvector, so is $-\mathbf{v}$.

Clearly, $\boldsymbol{RP^2}$is a model for line fields. While $\boldsymbol{RP^2}$is well known to geometers and has been used in physics, particularly for describing singularities in nematic crystals topologically, it has not used in DTI before. We propose to use it for both visualizing and analyzing the diffusion tensor fields, demonstrate its promise with preliminary results discussed in Section C.1.

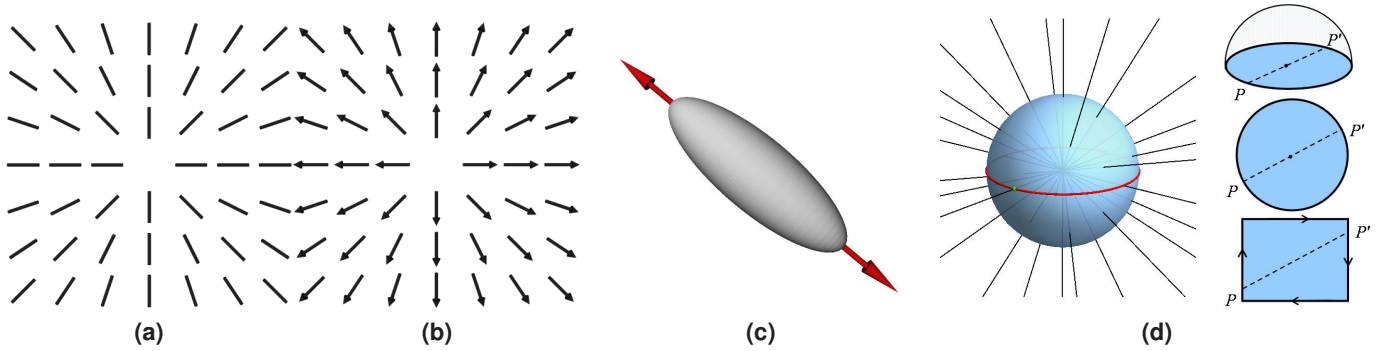

Figure 2: *a) A vector field. b) A line field. Sphere colored using c) The principal axis of a symmetric second order tensor gives a line, which is a point on $\boldsymbol{RP^2}$ d) Models of $\boldsymbol{RP^2}$. Top: The upper hemisphere, with antipodal points on the equator identified. Middle: a unit disk, with antipodal boundary points identified. Bottom: A rectangle, with opposite edges identified, with a reversal in orientation.*

B.4 Bayesian Resolving of Fiber Tract Crossings

One of the limitations of DTI is its assumption that single tensor can explain tissue orientation at a given voxel. In the brain, on the other hand, neural tracts cross (X), kiss (><), and branch (-<). In other words, use of single tensor model estimates local geometry inaccurately in these cases, often as an isotropic tensor. This limitation of the traditional tensor model has led to the development of different acquisition techniques along with more complex models of diffusion. One strategy to characterize the underlying complex fiber architecture is to quantify the diffusion function using the Fourier relationship first observed by Stejskal and Tanner [63], between the diffusion function and the diffusion signal attenuation in q-space [15]. Q-space imaging methods aim to directly measure the 3D probability diffusion function of water molecules. A number of approaches based on q-space imaging have been proposed recently [42, 67, 66, 65, 69]. These methods, however, require a large number of gradient directions (i.e., more than 100), incurring long acquisition times, which make them impractical in a clinical setting.

Therefore previous work has attempted to explicitly model the complexity of the DWI signal formation in the presence of multiple fibers [2]. A simple model is a mixture of Gaussian densities [1, 12], which can be thought of as a generalization of the single-tensor model. A similar approach by Behrens et al. modeled the underlying diffusion profile using infinite anisotropic components and a single isotropic component [7], resulting in a computational intensive optimization problem with non-linear constraints. Recently, Peled et al. introduced a constrained bi-Gaussian model for analysis of crossing fibers with fewer model parameters, utilizing the information present in the single tensor [53]. This two-tensor approach models a voxel containing two tracts using two cylindrical tensors (with identical eigenvalues), that lie in the plane spanned by the two largest eigenvectors of the single-tensor fit. Apparent goal of the restriction on the geometry is to simplify and speed up the fitting process.

Surprisingly, all these previous methods either ignore geometry and/or locality of it (i.e., neighborhood information). Neither they incorporate the model complexity into their fitting process in model selection.

We will pose the problem as a simple Bayesian model selection problem and solve for the ”optimum” number of tensors at each voxel using a hierarchical (i.e., hierarchy of different scales) Markov Random Field [8, 9, 29].

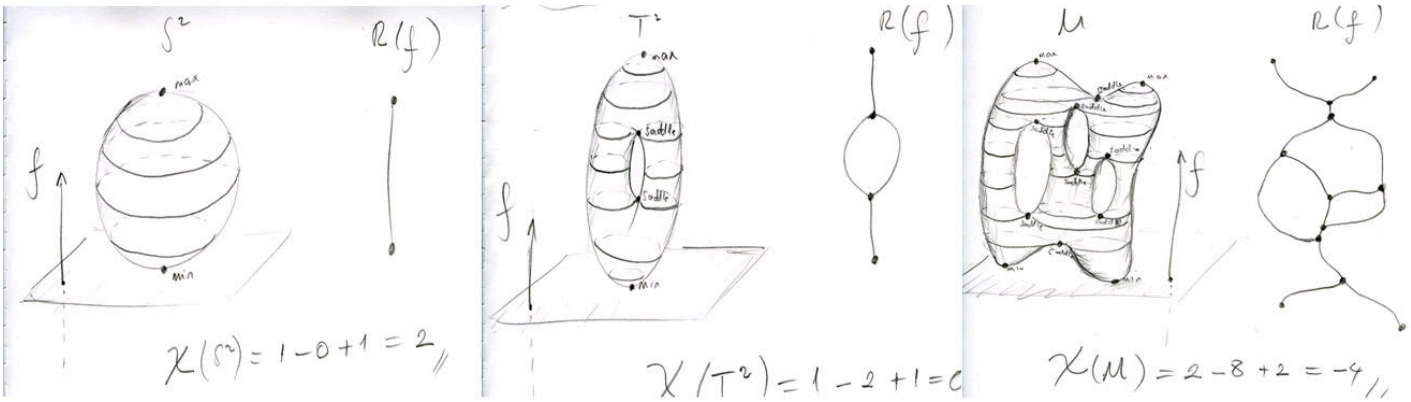

Figure 3: *Reeb graphs $R(f)$ of the height function f defined over three different surfaces of genus 0, 1, and 3, respectively.*

B.5 Reeb Graphs

Reeb graphs represent the connectivity of the level sets of functions defined over manifolds and are obtained by contracting the connected components of the level sets to a point [59, 56]. Under certain conditions (i.e., when the function is a Morse function and the space is a surface), Reeb graphs also encode the topology of the space over which the function is defined [20] (see Figure 3 for examples). Reeb graphs have been used extensively in a wide range of applications such as shape matching using hierarchical resolutions of shapes [38] and isotopic surface embedding [60], shape encoding [45, 64], compression [10], surface parametrization [62], iso-surface remeshing [72] and simplification [71], representation and visualization of time-varying volumetric simulation data [25]. Further discussion on Reeb graphs and applications can be found in [28, 10].

While Reeb grahs have been generally computed for functions over surfaces (2-manifolds) in the past, we are interested in functions defined over volumetric images (i.e., 3-manifolds with boundary). In this context, we propose to compute multi-scale Reeb graphs to represent and quantify the change in the brain connectivity. We are not aware of previous work. While initially, we will compute Reeb graphs of tensor invariants such FA and MD (i.e., scalar functions), we also aim to generalize Reeb graphs to higher dimensional functions defined over manifolds (e.g., doing something better than computing Reeb graph for each dimension separately for a vector-valued function).

B.6 Computational Homology for Qualitatively Capturing Structure in Data

> *Anyone who wishes to learn topology with an interest in its applications must begin with the Betti groups.* Pavel S. Alexandrov([3, 4]).

Are there any invariants (topological or otherwise) of the connectivity in the brain? If so, if and how do they change? This is somewhat the same question that we have been asking so far: What are the structures and patterns of connectivity in the brain that are invariant across subjects or even species (of close kin)?

Our goal is to represent the structure in the connectivity and its change with disease both quantitatively and qualitatively. Topology provides an important formalism for qualitatively characterizing the structure in data [3, 37, 35].

Like in any other systematic study of things, topology also concerns with the classification (or equivalence) of its subjects, which suggests a notion of invariance. A topological invariant is a property of the space which does not

change under topological isomorphisms (a.k.a. homeomorphism: a bijective continuous map inverse of which is also continuous). In broad terms, topological invariants do not change under continuous stretching and bending of the space without tear (hence the popular notion of topology as rubber sheet geometry). Examples of topological invariants include the Euler-Poincare characteristic, orientability, homology groups, homotopy groups, dimension, compactness, connectedness, and Hausdorfness.

As part of algebraic topology, homology theory studies n-dimensional cycles in topological spaces and invariants based on equivalence classes of cycles (homology classes) [30]. Homology theory resulted in many invariants; the basic one is the Betti numbers, ranks of free abelian groups (homology groups) formed by equivalence classes of cycles. Simplicial homology, homology over simplicial approximations of continuous spaces, provide tractable ways of computing homological invariants such as Betti numbers by means of linear algebra.

In his concise treatment of combinatorial topology [4], Pavel S. Alexandrov concludes his book by the indicating the great potential of Betti groups for applications. Following Alexandrov's lead, computational homology, based on mainly simplicial homology, has found interesting applications recently [31]. In a pioneering work, Edelsbrunner et al. introduced the persistent homology formalism to compute and record the Betti numbers of data points at varying filtrations. The resulting representation showing appearance and disappearance of the Betti numbers is called barcode. Zomorodian and Carlsson extended persistent homology, essentially a multiscale approach, to arbitrary spaces and field coefficients [75].

Carlsson et al. use persistent homology to analyze the topology of the space of natural images, a collection of 3 by 3 image patches pre-processed to be restricted to a seven-dimensional sphere (S^7) as described in [46]. The authors show that the underlying "persistent" space of natural images has the topology of Klein bottle [17].

In a similar spirit, Singh et al. apply persistent homology to the study of population activity in the primary visual cortex (V1) [61], showing the space of the activity patterns has the topology of two-sphere (S^2).

We propose to compute the persistent homology barcodes of DTI data for ROIs in brain and quantify their change with disease, by directly comparing the barcodes. We are not aware of any previous work applying similar ideas in the brain connectivity setting.

C Preliminary Work

We discuss below three works in line of our proposal. The first work application of using $\boldsymbol{RP^2}$as a model of line fields. One of the common ways of visualizing tensor fields is to colormap the dominant orientation of the tensor (i.e., the principal axis), collection of which constitutes a line field, at each point. We use an immersion of the real projective plane ($\boldsymbol{RP^2}$), which we proposed as a model of line fields in section A.2, for one-to-one, continuous coloring of line fields. We show examples from coloring cross-sections and integral curves of DTI brain data sets [21].

The second work combines an intuitive geometric idea (i.e., slicing) with statistical machine learning techniques. While the presented application assess the stability of clusterings for DTI integral curves, the method can be used embedding curves into the plane regularly [22]. This will help in automatically creating two-dimensional connectivity diagrams that we proposed in section A.1.

The third work is also related to the proposed idea in Section A.1 in the sense that representing and interacting with the brain connectivity using two dimensional maps.

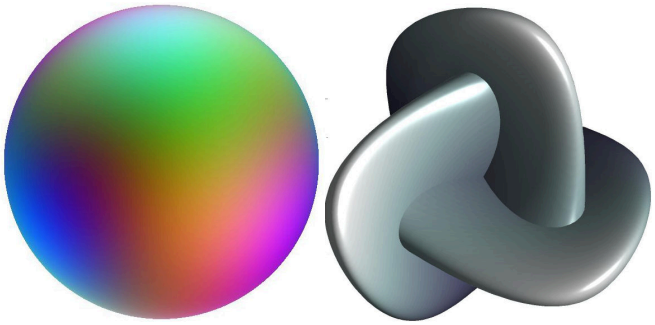

Figure 4: *a) Sphere colored by immersing $\boldsymbol{RP^2}$ in RGB color space b) Boy's surface*

C.1 Coloring 3D line fields using Boy's real projective plane immersion

It is often useful to visualize a *line field*, a function that sends each point P of the plane or of space to a line through P; such fields arise in the study of tensor fields, where the principal eigendirection at each point determines a line (but not a vector, since if $\mathbf{v}$ is an eigenvector, so is $-\mathbf{v}$). To visualize such a field, we often assign a color to each line; thus we consider the coloring of line fields as a mapping from the real projective plane ($\boldsymbol{RP^2}$) to color space. Ideally, such a coloring scheme should be smooth and one-to-one, so that the color uniquely identifies the line; unfortunately, there is not such mapping because $\boldsymbol{RP^2}$, like any other closed non-orientable manifold, admits no embedding in $\mathbf{R^3}$. We introduce Boy's surface (see Figure 4) [14], an immersion of the projective plane in 3D, as a model for coloring line fields, and show results from its application in visualizing orientation in diffusion tensor fields. This coloring method is smooth and one-to-one except on a set of measure zero (the double curve of Boy's surface). A complete discussion of this work can be found in [21].

C.2 A slicing-based coherence measure for clusters of DTI integral curves

Reflecting the intricacy of the connectivity in the brain, three dimensional tractography models (dense collections of curves obtained via fiber-tracking) are generally visually dense making it difficult for experts to ascertain anatomical and functional structures clearly. Therefore, there is a considerable interest in developing effective clustering methods.

In this context, we introduce a measure of coherence for a "hypothesized" cluster of curves. The cluster coherence measure we propose relies on evaluating the stability of further subdivision of the cluster. To this end, we use the configurations at what we call "slices"– cross-sections of the cluster(see Figure 6). Each slice is effectively an embedding of the curves into points in two-dimensional space. These points can be clustered using any off-the-shelf clustering algorithm. Each slice therefore provides a "vote" for each pair of curves being together or separate in the overall clustering. Furthermore, assuming reasonable smoothness of the curves, we can assess the temporal coherence of these votes: two adjacent slices carry more weight voting the same way than if their votes are opposite.

We demonstrate our measure's use to improve an agglomerative hierarchical clustering algorithm that has been shown to be working relatively well in clustering integral curves corresponding neurofibers [48]. When our slice-based method detects that a stable split exists in the cluster, it provides a specific partitioning, that can be used as part of a clustering algorithm. Expert evaluation shows that this mechanism may be superior to the standard hierarchical clustering approach. While our primary motivation in designing the slicing-based coherence

measure is the task of refining an initial clustering assignment, it can be used for validating clusterings, quantifying connectivity or parametrizing clusters. Further details of this work can be found in [22].

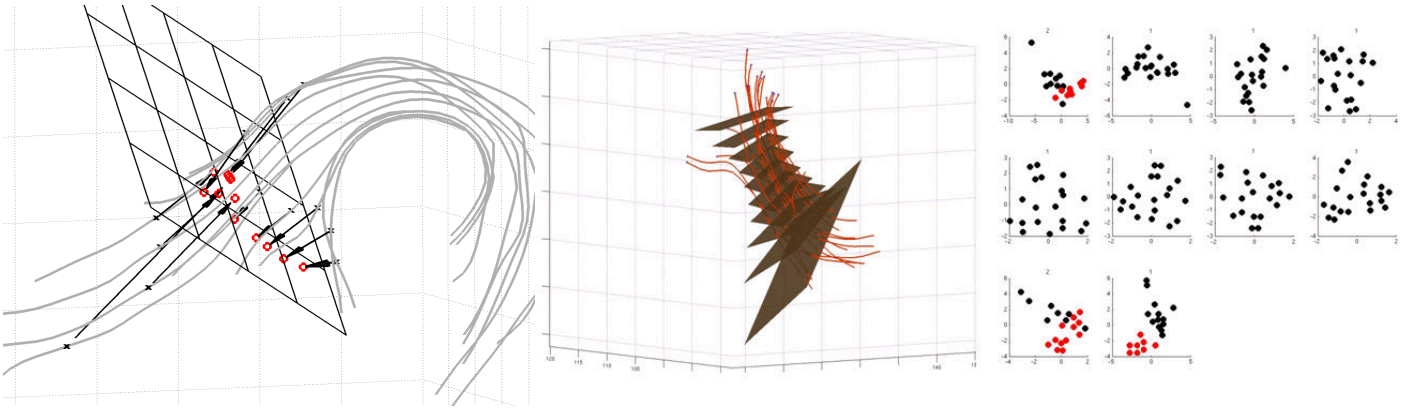

(a) **(b)**

Figure 5: *Illustration: a) A cluster of fiber tracts is sliced at the arc length ratio $\alpha = 0.2$. Crosses (black): points on the curve corresponding to the arc length parameter αS_i. Circles (red): projections on the slicing plane. b) Another cluster sliced at 10 different points. Each planar point set indicates the embedding of the cluster in the axis-aligned plane of the corresponding slice. Point sets are also clustered using a Gaussian mixture model to be incorporated in our cluster stability measure.*

C.3 Exploring 3D DTI Fiber Tracts with Linked 2D Representations

We introduce a visual exploration paradigm that facilitates navigation through complex fiber tracts by combining traditional 3D model viewing with 2D representations. To this end, we create standard streamtube models along with an embedding in the plane for a given set of fiber tracts. We then link these representations using both interaction and color obtained by embedding fiber tracts into a perceptually uniform color space. We conducted an anecdotal evaluation with neuroscientists to assess the usefulness of our method in exploring anatomical and functional structures in the brain. Expert feedback indicates that, while a standalone clinical use of the proposed method would require anatomical landmarks in the lower dimensional representations, the approach would be particularly useful in accelerating tract bundle selection. Results also suggest that combining traditional 3D model viewing with lower dimensional representations can ease navigation through the complex fiber tract models, improving exploration of the connectivity in the brain. Details of our preliminary work can be found in [44].

What is proposed in Section A.1 can be thought as extension of the work discussed above: While we represent each tract with a single 2D point , in section we propose to represent each with two 2D points corresponding to the ends of the tract and a path between them obeying a set of anatomical and visual constraints.

D Timeline

Year 1:

* Implement Bayesian model selection for diffusion tensor fitting.

Figure 6: *Fiber tracts computed from a DTI whole brain data set (upper-left). The corpus callosum (colored red) is selected through a 2D embedding of the fiber tracts (upper-right). The selection is also indicated in a hierarchical clustering tree of the fiber tracts (lower-left). Tracts and their corresponding points in lower-dimensional representations are colored by embedding the tracts in three dimensional space of L*a*b* color model (lower-right).*

* Compare the fiber-tracking results based on this new fitting with the state of the art in the optic chiasm in the brain.
* Develop software infrastructure for geometry processing.
* Implement Reeb graph construction on diffusion tensor invariants.
* Implement Betti number computation on simplicial complexes.

Year 2:

* Generalize Reeb graphs to vector-valued functions.
* Formulate stability of the Reeb graphs.
* Generate 2d connectivity diagrams for the clustered dti curves.
* Generate 2d connectivity diagrams for the clustered dti curves with neo-cortex projection labels.
* Evaluate usefulness the results with experts.

References

[1] ALEXANDER, A. L., HASAN, K. M., LAZAR, M., TSURUDA, J. S., AND PARKER, D. L. Analysis of partial volume effects in diffusion-tensor mri. *Magnetic Resonance in Medicine 45*, 5 (May 2001), 770–780.

[2] ALEXANDER, D. C. Multiple-fiber reconstruction algorithms for diffusion mri. *Annals of the New York Academy of Sciences 1064* (Dec. 2005), 113–133.

[3] ALEXANDROFF, P. *Elementary Concepts of Topology*. Dover, 1961.

[4] ALEXANDROV, P. S. *Einfachste Grundbegriffe der Topologie*. Julius Springer, 1932.

[5] BASSER, P. J., AND JONES, D. K. Diffusion-tensor mri: theory, experimental design and data analysis - a technical review. *NMR in Biomedicine 15* (2002), 456–467.

[6] BEHRENS, T. E., JOHANSEN-BERG, H., WOOLRICH, M. W., SMITH, S. M., WHEELER-KINGSHOTT, C. A., BOULBY, P. A., BARKER, G. J., SILLERY, E. L., SHEEHAN, K., CICCARELLI, O., THOMPSON, A. J., BRADY, J. M., AND MATTHEWS, P. M. Non-invasive mapping of connections between human thalamus and cortex using diffusion imaging. *Nat Neurosci 6*, 7 (2003), 750–7. 1097-6256 (Print)Journal Article.

[7] BEHRENS, T. E., WOOLRICH, M. W., JENKINSON, M., JOHANSEN-BERG, H., NUNES, R. G., CLARE, S., MATTHEWS, P. M., BRADY, J. M., AND SMITH, S. M. Characterization and propagation of uncertainty in diffusion-weighted mr imaging. *Magn Reson Med 50*, 5 (2003), 1077–88. Journal ArticleResearch Support, Non-U.S. Gov'tUnited Statesofficial journal of the Society of Magnetic Resonance in Medicine / Society of Magnetic Resonance in Medicine.

[8] BESAG, J. Spatial interaction and the statistical analysis of lattice systems. *Journal of the Royal Statistical Society: Series B 36* (1974), 192–236.

[9] BESAG, J. On the statistical analysis of dirty pictures. *Journal of the Royal Statistical Society. Series B (Methodological) 48*, 3 (1986), 259–302.

[10] BIASOTTI, S., GIORGI, D., SPAGNUOLO, M., AND FALCIDIENO, B. Reeb graphs for shape analysis and applications. *Theor. Comput. Sci. 392*, 1-3 (2008), 5–22.

[11] BIHAN, D. L., MANGIN, J.-F., POUPON, C., CLARK, C. A., PAPPATA, S., MOLKO, N., AND CHABRIAT, H. Diffusion tensor imaging: Concepts and applications. *Journal of Magnetic Resonance Imaging 13* (2001), 534–546.

[12] BLYTH, R., COOK, P. A., AND ALEXANDER, D. C. Tractography with multiple fibre directions. In *Proceedings of the 11th Scientific Meeting of the International Society for Magnetic Resonance in Medicine* (2003), p. 240.

[13] BOLTYANSKII, V., AND EFREMOVICH, V. *Intuitive Combinatorial Topology*. Springer-Verlag New York, 2000.

[14] BOY, W. *Über die Curvatura Integra und dieTopologie der Geschlossener Flachen*. PhD thesis, Universität Göttingen, Göttingen, 1901.

[15] CALLAGHAN, P. T., ECCLES, C. D., AND XIA, Y. Nmr microscopy of dynamic displacements: k-space and q-space imaging. *Journal of Physics E: Scientific Instruments 21*, 8 (1988), 820–822.

[16] CARLSSON, G. Topology and data. *Bull. Amer. Math. Soc. 46*, 2 (2009), 255–308.

[17] CARLSSON, G., ISHKHANOV, T., DE SILVA, V., AND ZOMORODIAN, A. On the local behavior of spaces of natural images. *International Journal of Computer Vision 76*, 1 (2008), 1–12.

[18] CATANI, M., HOWARD, R., PAJEVIC, S., AND JONES, D. Virtual in vivo interactive dissection of white matter fasciculi in the human brain. *NeuroImage 17:1* (2002), 77–94.

[19] CHABRIAT, H., PAPPATA, S., POUPON, C., CLARK, C. A., VAHEDI, K., POUPON, F., MANGIN, J.-F., PACHOT-CLOUARD, M., JOBERT, A., LEBIHAN, D., AND BOUSSER, M.-G. Clinical severity in CADASIL related to ultrastructural damage in white matter: in vivo study with diffusion tensor mri. *Stroke 30*, 12 (1999), 2637–2643.

[20] COLE-MCLAUGHLIN, K., EDELSBRUNNER, H., HARER, J., NATARAJAN, V., AND PASCUCCI, V. Loops in reeb graphs of 2-manifolds. In *SCG '03: Proceedings of the nineteenth annual symposium on Computational geometry* (New York, NY, USA, 2003), ACM, pp. 344–350.

[21] DEMIRALP, C., HUGHES, J. F., AND LAIDLAW, D. H. Coloring 3d line fields using boy's real projective plane immersion. In *Proceedings of IEEE Visualization* (2009).

[22] DEMIRALP, C., SHAKHNAROVICH, G., ZHANG, S., AND LAIDLAW, D. H. Slicing-based coherence measure for refining clusters of 3D curves. In *Proceedings of MICCAI* (2008).

[23] DU, A. T., SCHUFF, N., AMEND, D., LAAKSO, M. P., HSU, Y. Y., JAGUST, W. J., YAFFE, K., KRAMER, J. H., REED, B., NORMAN, D., CHUI, H. C., AND WEINER, M. W. Magnetic resonance imaging of the entorhinal cortex and hippocampus in mild cognitive impairment and alzheimer's disease. *J Neurol Neurosurg Psychiatry 71*, 4 (October 2001), 441–447.

[24] EDELSBRUNNER, H., AND HARER, J. Persistent homology–a survey, 2008.

[25] EDELSBRUNNER, H., HARER, J., MASCARENHAS, A., PASCUCCI, V., AND SNOEYINK, J. Time-varying reeb graphs for continuous space–time data. *Comput. Geom. Theory Appl. 41*, 3 (2008), 149–166.

[26] ELLIS, C. M., SIMMONS, A., JONES, D. K., BLAND, J., DAWSON, J. M., HORSFIELD, M. A., WILLIAMS, S. C., AND LEIGH, P. N. Diffusion tensor mri assesses corticospinal tract damage in als. *Neurology 53*, 5 (September 1999), 1051–1058.

[27] FILIPPI, C. G., ULUG, A. M., RYAN, E., FERRANDO, S. J., AND VAN GORP, W. Diffusion tensor imaging of patients with hiv and normal-appearing white matter on mr images of the brain. *American Journal of Neuroradiology 22* (February 2001), 277–283.

[28] FOMENKO, A. T., AND KUNII, T. L., Eds. *Topological Methods for Visualization*. Tokyo, Japan, Springer-Verlag, 1997.

[29] GEMAN, S., AND GEMAN, D. Stochastic relaxation, gibbs distributions and the bayesian restoration of images. *IEEE Trans. Pattern Anal. Machine Intell. 6* (1984), 721–741.

[30] GIBLIN, P. J. *Graphs, Surfaces and Homology: An Introduction to Algebraic Topology*, 2nd ed. Chapman and Hall, 1981.

[31] GIHRIST, R. Three examples of applied and computational homology. *The Nieuw Archief voor Wiskunde 5/0*, 2 (2008), 122–125.

[32] GRAHAM, J. M., PAPADAKIS, N., EVANS, J., WIDJAJA, E., ROMANOWSKI, C., PALEY, M., WALLIS, L. I., WILKINSON, I., SHAW, P. J., AND GRIFFITHS, P. D. Diffusion tensor imaging for the assessment of upper motor neuron integrity in als. *Neurology 63* (20-4), 2111–2119.

[33] HAGMANN, P., CAMMOUN, L., GIGANDET, X., MEULI, R., HONEY, C. J., WEDEEN, V. J., AND SPORNS, O. Mapping the structural core of human cerebral cortex. *PLoS Biology 6*, 7 (July 2008), e159+.

[34] HANYU, H., ASANO, T., SAKURAI, H., IMON, Y., IWAMOTO, T., TAKASAKI, M., SHINDO, H., AND ABE, K. Diffusion-weighted and magnetization transfer imaging of the corpus callosum in alzheimer's disease. *Journal of the neurological sciences 167*, 1 (August 1999), 37–44.

[35] HATCHER, A. *Algebraic Topology*. Cambridge Press, 2002.

[36] HE, Y., CHEN, Z. J. J., AND EVANS, A. C. C. Small-world anatomical networks in the human brain revealed by cortical thickness from mri. *Cereb Cortex* (January 2007).

[37] HENLE, M. *A Combinatorial Introduction to Topology*. Dover, 1994.

[38] HILAGA, M., SHINAGAWA, Y., KOHMURA, T., AND KUNII, T. L. Topology matching for fully automatic similarity estimation of 3d shapes. In *SIGGRAPH '01: Proceedings of the 28th annual conference on Computer graphics and interactive techniques* (New York, NY, USA, 2001), ACM, pp. 203–212.

[39] HORSFIELD, M. A., LAI, M., AND WEBB, S. Apparent diffusion coefficients in benign and secondary progressive multiple sclerosis by nuclear magnetic resonance. *Magn. Reson. Med. 36* (1996), 393–400.

[40] ITURRIA-MEDINA, Y., CANALES-RODRIGUEZ, E. J., MELIE-GARCIA, L., VALDES-HERNANDEZ, P. A., MARTINEZ-MONTES, E., ALEMAN-GOMEZ, Y., AND SANCHEZ-BORNOT, J. M. Characterizing brain anatomical connections using diffusion weighted mri and graph theory. *NeuroImage 36*, 3 (2007), 645–660.

[41] ITURRIA-MEDINA, Y., SOTERO, R. C., CANALES-RODRIGUEZ, E. J., ALEMAN-GOMEZ, Y., AND MELIE-GARCIA, L. Studying the human brain anatomical network via diffusion-weighted mri and graph theory. *NeuroImage 40*, 3 (2008), 1064–1076.

[42] JANSONS, K. M., AND ALEXANDER, D. C. Persistent angular structure: new insights from diffusion magnetic resonance imaging data. *Inverse Problems 19*, 5 (2003), 1031–1046.

[43] JIAN, B., AND VEMURI, B. C. Multi-fiber reconstruction from diffusion mri using mixture of wisharts and sparse deconvolution. In *IPMI* (2007), N. Karssemeijer and B. P. F. Lelieveldt, Eds., vol. 4584 of *Lecture Notes in Computer Science*, Springer, pp. 384–395.

[44] JIANU, R., DEMIRALP, C., AND LAIDLAW, D. H. Exploring 3d dti fiber-tracts with linked 2d representations. In *Proceedings of IEEE Visualization* (2009). In Press.

[45] LAZARUS, F., AND VERROUST, A. Level set diagrams of polyhedral objects. In *SMA '99: Proceedings of the fifth ACM symposium on Solid modeling and applications* (New York, NY, USA, 1999), ACM, pp. 130–140.

[46] LEE, A. B., PEDERSEN, K. S., AND MUMFORD, D. The nonlinear statistics of high-contrast patches in natural images. *Int. J. Comput. Vision 54*, 1-3 (2003), 83–103.

[47] MILO, R., ITZKOVITZ, S., KASHTAN, N., LEVITT, R., SHEN-ORR, S., AYZENSHTAT, I., SHEFFER, M., AND ALON, U. Superfamilies of evolved and designed networks. *Science 303*, 5663 (March 2004), 1538–1542.

[48] MOBERTS, B., VILANOVA, A., AND VAN WIJK, J. J. Evaluation of fiber clustering methods for diffusion tensor imaging. In *Procs. of Vis'05* (2005), pp. 65–72.

[49] MOLKO, N., PAPPATA, S., MANGIN, J.-F., POUPON, F., BIHAN, D. L., BOUSSER, M. G., AND CHABRIAT, H. Monitoring disease progression in CADASIL with diffusion magnetic resonance imaging: a study with whole brain histogram analysis. *Stroke 33*, 12 (2002), 2902–2908.

[50] MORI, S., AND ZHANG, J. Principles of diffusion tensor imaging and its applications to basic neuroscience research. *Neuron 51* (2006), 527–539.

[51] MOSELEY, M. E., COHEN, Y., MINTOROVITCH, J., CHILEUITT, L., SHIMIZU, H., KUCHARCZYK, J., WENDLAND, M. F., AND WEINSTEIN, P. R. Early detection of regional cerebral ischemia in cats: Comparison of diffusion- and t2-weighted mri and spectroscopy. *Magnetic Resonance in Medicine 176* (1990), 330–346.

[52] NEIL, J., MILLER, J., MUKHERJEE, P., AND HÜPPI, P. S. Diffusion tensor imaging of normal and injured developing human brain - a technical review. *NMR in Biomedicine 15*, 7-8 (2002), 543–552.

[53] PELED, S., FRIMAN, O., JOLESZ, F., AND WESTIN, C.-F. Geometrically constrained two-tensor model for crossing tracts in DWI. *Magnetic Resonance Imaging 24* (2006), 1263–1270.

[54] POMARA, N., CRANDALL, D., CHOI, S., JOHNSON, G., AND LIM, K. White matter abnormalities in HIV-1 infection: a diffusion tensor imaging study. *Psychiatry Res 106*, 1 (2001), 15–24.

[55] RAGIN, A. B., STOREY, P., COHEN, B. A., EPSTEIN, L. G., AND EDELMAN, R. R. Whole brain diffusion tensor imaging in hiv-associated cognitive impairment. *AJNR Am. J. Neuroradiol. 25*, 2 (2004), 195–200.

[56] REEB, G. Sur les points singuliers d'une forme de Pfaff complétement intégrable ou d'une fonction numérique[on the singular points of a completely integrable pfaff form or of a numerical function]. *Comptes Rendus de L'Académie ses Sciences* (1946), 847–849.

[57] ROSEA, S. E., CHENA, F., CHALKB, J. B., ZELAYAD, F. O., STRUGNELLC, W. E., BENSONC, M., SEMPLEE, J., AND DODDRELLA, D. M. Loss of connectivity in alzheimer's disease: an evaluation of white matter tract integrity with colour coded mr diffusion tensor imaging. *J Neurol Neurosurg Psychiatry 69* (2000), 528–530.

[58] SACH, M., WINKLER, G., GLAUCHE, V., LIEPERT, J., HEIMBACH, B., KOCH, M. A., BUCHEL, C., AND WEILLER, C. Diffusion tensor mri of early upper motor neuron involvement in amyotrophic lateral sclerosis. *Brain 127(2)* (2004), 340–350.

[59] SHINAGAWA, Y., AND KUNII, T. L. Constructing a reeb graph automatically from cross sections. *IEEE Comput. Graph. Appl. 11*, 6 (1991), 44–51.

[60] SHINAGAWA, Y., KUNII, T. L., AND KERGOSIEN, Y. L. Surface coding based on morse theory. *IEEE Computer Graphics and Applications 11*, 5 (1991), 66–78.

[61] SINGH, G., MEMOLI, F., ISHKHANOV, T., SAPIRO, G., CARLSSON, G., AND RINGACH, D. L. Topological analysis of population activity in visual cortex. *J. Vis. 8*, 8 (6 2008), 1–18.

[62] STEINER, D., AND FISCHER, A. Cutting 3d freeform objects with genus-n into single boundary surfaces using topological graphs. In *SMA '02: Proceedings of the seventh ACM symposium on Solid modeling and applications* (New York, NY, USA, 2002), ACM, pp. 336–343.

[63] STEJSKAL, E. O., AND TANNER, J. E. Spin diffusion measurements: Spin echoes in the presence of a time-dependent field gradient. *Journal of Chemical Physics 42*, 1 (January 1965), 288–292.

[64] TAKAHASHI, S., SHINAGAWA, Y., AND KUNII, T. L. A feature-based approach for smooth surfaces. In *SMA '97: Proceedings of the fourth ACM symposium on Solid modeling and applications* (New York, NY, USA, 1997), ACM, pp. 97–110.

[65] TOURNIER, CALAMANTE, F., GADIAN, D. G., AND CONNELLY, A. Direct estimation of the fiber orientation density function from diffusion-weighted mri data using spherical deconvolution. *NeuroImage 23*, 3 (November 2004), 1176–1185.

[66] TUCH, D. S. Q-ball imaging. *Magnetic Resonance in Medicine 52*, 6 (2004), 1358–1372.

[67] TUCH, D. S., REESE, T. G., WIEGELL, M. R., AND WEDEEN, V. J. Diffusion mri of complex neural architecture. *Neuron 40*, 5 (2003), 885 – 895.

[68] WANG, Y., ZHANG, J., MORI, S., AND NATHANS, J. Axonal growth and guidance defects in frizzled3 knock-out mice:a comparison of diffusion tensor magnetic resonance imaging, neurofilament staining, and genetically directed cell labeling. *J. Neurosci. 26(2)* (2006), 355–364.

[69] WEDEEN, V. J., , REESE, T. G., TUCH, D. S., WIEGELL, M. R., DOU, J.-G., WEISKOFF, R., AND CHESSLER, D. Mapping fibre orientation spectra in cerebral white matter with fourier-transform diffusion mri. In *Proceedings of ISMRM* (2000), p. 82.

[70] WERRING, D. J., BRASSAT, D., DROOGAN, A. G., CLARK, C. A., SYMMS, M. R., BARKER, G. J., MACMANUS, D. G., THOMPSON, A. J., AND MILLER, D. H. The pathogenesis of lesions and normal-appearing white matter changes in multiple sclerosis: a serial diffusion mri study. *Brain 123 (Pt 8)* (Aug 2000), 1667–1676.

[71] WOOD, Z., HOPPE, H., DESBRUN, M., AND SCHRÖDER, P. Removing excess topology from isosurfaces. *ACM Trans. Graph. 23*, 2 (2004), 190–208.

[72] WOOD, Z. J., SCHRÖDER, P., BREEN, D., AND DESBRUN, M. Semi-regular mesh extraction from volumes. In *VIS '00: Proceedings of the conference on Visualization '00* (Los Alamitos, CA, USA, 2000), IEEE Computer Society Press, pp. 275–282.

[73] ZHANG, J., CHEN, Y.-B., HARDWICK, M. J., MILLER, M. I., PLACHEZ, C., RICHARDS, L. J., YAROWSKY, P., VAN ZIJL, P., AND MORI, S. Magnetic resonance diffusion tensor microimaging reveals a role for bcl-x in brain development and homeostasis. *J. Neurosci. 25*, 8 (February 2005), 1881–1888.

[74] ZHANG, J., RICHARDS, L. J., MILLER, M. I., YAROWSKY, P., VAN ZIJL, P., AND MORI, S. Characterization of mouse brain and its development using diffusion tensor imaging and computational techniques. In *Proceedings of IEEE EMBC* (2006), pp. 2252–2255.

[75] ZOMORODIAN, A., AND CARLSSON, G. Computing persistent homology. *Discrete & Computational Geometry 33*, 2 (2005), 249–274.